

# Large to intermediate-scale aquifer heterogeneity in fine-grain dominated alluvial fans (Cenozoic As Pontes Basin, northwestern Spain): Insight based on 3-dimensional geostatistical reconstruction

FALIVENE, O., CABRERA, L., AND SÁEZ, A.

*Department of Stratigraphy, Paleontology and Marine Geosciences. Group of Geodynamics and Basin Analysis. Geomodels Institute. Facultat de Geologia. Universitat de Barcelona. c/ Martí i Franquès s/n, 08028 Barcelona*

Corresponding author: FALIVENE, O.

Mail address: orioalfalivene@ub.edu, tel: +34 93 403 4028, fax: +34 93 402 1370

**Abstract:** Facies reconstructions are used in hydrogeology to improve the interpretation of aquifer permeability. In the absence of sufficient data to define the heterogeneity due to geological processes, uncertainties in the distribution of aquifer hydrofacies and characteristics may appear. Geometric and geostatistical methods are used to understand and model aquifer hydrofacies distribution, providing models to improve comprehension and development of aquifers. However, these models require some input statistical parameters that can be difficult to infer from the study site. A 3D reconstruction of a kilometer scale fine-grain dominated Cenozoic alluvial fan derived from a large number of continuously cored, closely spaced, and regularly distributed wells is presented. The facies distributions were reconstructed using a genetic stratigraphic subdivision and a deterministic geostatistical algorithm. The reconstruction is slightly affected by variations in the geostatistical input parameters because of the high-density data set. Analysis of the reconstruction allowed identification in the proximal to medial alluvial fan zones of several laterally extensive sand bodies with relatively higher permeability; these sand bodies were quantified in terms of volume, mean thickness, maximum area, and maximum equivalent diameter. These quantifications provide trends and geological scenarios for input statistical parameters to model aquifer systems in similar alluvial fan depositional settings.

**Keywords:** *fine-grained alluvial fan, statistical facies modeling, geostatistics, heterogeneity, geometric parameters.*

# Introduction

## ***Sedimentary analogues***

The compilation of databases quantifying facies evolutionary trends and geometrical/geostatistical parameters in depositional units is a major research issue (i.e. Falkner and Fielding 1993; Bryant and Flint 1993; Dreyer et al. 1993; Robinson and McCabe 1997; Hornung and Aigner 1999; Tye 2004; de Marsily et al. 2005), and can be achieved in locations where these units are especially accessible, exposed, or sampled. These units are also referred to as analogues (i.e. exceptional outcrop/field exposures, extensively drilled zones, or modern depositional environments). Trends and parameters derived from analogues can be used as scenarios for input statistical parameters (i.e. geometric dimensions or variograms) in studies when the sampling density is not enough to capture the entire spatial variability because of the short-scale variations in sedimentary facies. Nevertheless, realistic models reproducing the spatial variability of facies are necessary to provide control over the uncertainty in facies correlations, and stochastic simulation is applied with either object-based or geostatistical methods (i.e. Haldorsen and Damsleth 1990; Deutsch and Hewett 1996; Koltermann and Gorelick 1996; Webb and Davis 1998; de Marsily et al. 1998; Kupfersberger and Deutsch 1999; de Marsily et al. 2005; Falivene et al. 2006a and 2006b). In siliciclastic aquifers, the use of realistic facies models to guide the modeling of porosity and permeability improves predictions, because these parameters are commonly correlated with facies (Anderson 1989; Jussel et al. 1994; Ritzi et al. 1995; Fogg et al. 1998; Gómez-Hernández and Deutsch 1999).

## ***Fine-grain dominated alluvial fans***

Quantification and modeling of the heterogeneity in Recent to Cenozoic alluvial fan alluvial fan successions constitute significant aims given their importance in groundwater resources (e.g. Johnson and Driess 1989; Johnson 1995; Carle et al. 1998; Weissmann et al. 1999; Weissmann and Fogg alluvial fan 1999; Weissmann et al. 2002). Most of the descriptions and analyses of alluvial fans have focused on systems characterized by widespread proximal to medial coarse-grain facies, given their ubiquity in many climatic and tectonic settings (Fraser and Suttner 1986; Nemeč and Steel 1988; Harvey 1989; Rachocki and Church 1990; Bull 1991; Blair and MacPherson 1994; Miall 1996). Oppositely, fine-grain dominated alluvial fans are less widespread and less well documented than coarse-grain dominated fans. Nevertheless, fine-grain dominated alluvial fans are frequently present and their generation is enhanced in climatic and tectonic settings where rock weathering in the catchments mainly yields mud-sized particles (Bull 1964a and 1964b; Legget et al. 1966; Campbell 1998; Nakayama 1996 and 1999; Blair 2003). The trends of hydrofacies distribution in fine-grain dominated alluvial fans have not been extensively described because of exposure limitations and lack of subsurface data (e.g. Bull 1964a and 1964b; Legget et al. 1966; Campbell 1998; Nakayama 1999).

## ***Purpose and Scope***

This paper deals with a large to intermediate-scale reconstruction of the hydrofacies distribution within a kilometre scale fine-grain dominated alluvial fan in the Cenozoic As Pontes Basin (northwestern Spain). The purpose of this paper is to document the three-dimensional geostatistical deterministic reconstruction of this alluvial fan, departing from closely spaced wells. The analysis of the reconstruction, combined with surface observations, enabled better understanding and characterization of the heterogeneity of sand hydrofacies

and provides trends and quantitative parameters describing the laterally extensive sand bodies that can be potentially used to derive geological scenarios for the stochastic modelling of less-constrained similar or analogue alluvial fan systems.

## **Geological setting**

### ***General basin features***

The Tertiary As Pontes Basin (northwestern Spain) is a small non-marine basin (12 km<sup>2</sup>) associated with an Oligocene-Early Miocene strike-slip fault system, which relates to the western onshore end of the Pyrenean belt, as shown in [Figures 1a and b](#). The basin basement and ancient catchment zones are made up mainly by major slates and schists, and minor quartzites and gneisses of Precambrian and Paleozoic age, which were intensely deformed during the Variscan orogeny ([Manera et al. 1979](#); [Santanach et al. 1988](#); [Bacelar et al. 1988](#); [Barsó et al., 2003](#); [Santanach et al., 2005](#); [Figure 1b](#)). The basin evolution started as a compressive underlapping step over, with the development of two isolated subbasins bounded by E-W oriented thrusts and N-S normal faults. Both subbasins merged into a single depositional area during the subsequent generation of a double restraining bend ([Ferrús 1998](#); [Santanach et al. 2005](#)). [Figure 1c](#) shows sketches of three significant basin evolution episodes displaying their main tectonic structures and the associated depositional environments.

The general paleoclimatic conditions during the development of the basin fill have been inferred from paleobiological and sedimentological data ([Medús 1965a and 1965b](#); [Menéndez Amor 1975](#); [Baltuille et al. 1992](#); [Cabrera et al. 1994 and 1995](#); [Sáez and Cabrera 2002](#); [Cavagnetto 2002](#)). The paleoclimate was subtropical, warmer than in the present and with dry and rainy seasons. High frequency humid-subhumid cycles characterized the basin evolution ([Sáez and Cabrera 2002](#)).

## ***Stratigraphy and depositional systems of the basin fill***

The sedimentary basin fill was syntectonic and resulted from the interaction of sedimentation in alluvial fans and lacustrine to marsh-swamp systems (Figure 1c; Cabrera et al. 1995 and 1996). Consequently, the basin infill consists of major siliciclastic alluvial facies assemblages together with significant brown coal deposits, as displayed in the longitudinal sketch of the basin in Figure 1d (Bacelar et al. 1988; Cabrera et al. 1995 and 1996; Ferrús 1998; Falivene et al. in press a). Because of its economic interest as a coal basin, the basin infill has been extensively drilled; Figure 2a shows well locations in the studied intervals.

The basin infill has been split into five major genetic stratigraphic units (Figure 1d). Genetic units 2 to 5 are formed by several composite sequences, which have been defined based on sequence stratigraphic concepts applied to continental deposits, and are bounded by isochronous or near-isochronous bottom and top surfaces related to the settling and spreading of the major coal seams (Ferrús 1998; Sáez and Cabrera 2002; Sáez et al. 2003; Figure 1d). Each sequence consists of two intervals: 1<sup>st</sup>) a lower, areally restricted alluvial-fan interval (labeled interval A), where the siliciclastic successions interfinger with marsh-swamp coals and coaly mudstones; and 2<sup>nd</sup>) an upper, areally spread alluvial-fan interval (labeled interval B), composed exclusively of siliciclastics.

Mudstone, sand, and very minor fine-grained conglomerate make up most of the As Pontes Basin alluvial-fan successions. The widespread predominance of mudstone and sandy mudstone facies show that fine-grained sediments fed these systems predominantly. The rock composition of the basin catchment (major slates and schists and minor quartzites and gneisses; Figure 1b; Barsó et al. 2003; Sáez et al. 2003), and the warm and humid-subhumid paleoclimatic conditions (Medús 1965a and 1965b; Menéndez Amor 1975; Baltuille et al. 1992; Cabrera et al. 1994; Cavagnetto 2002) account for this predominance.

The low frequency alternation of areally restricted versus areally spread alluvial fan intervals, that characterizes most of the basin fill, was mainly tectonic in origin, because of variations on subsidence and sediment input rates. Episodes of more intense tectonic activity in the basin were characterized by high subsidence rates, and resulted in the alluvial fans retrogradation and restriction to the basin margin zones. Oppositely, episodes of relative tectonic quiescence gave rise to low subsidence rates that coupled in some cases with larger detritic inputs, and resulted in basinward progradation of the alluvial fan deposits (Ferrús 1998; Santanach et al. 2005).

### ***Alluvial fan facies in sequence 13***

The upper part of Unit 3 is made up by sequence 13. This unit was chosen for hydrofacies geostatistical reconstruction because it records one of the largest expansions of alluvial fan deposits during the basin evolution (Figure 1d). Such a large alluvial fan expansion was triggered both by a long-term drainage back spreading in the basin catchment (Sáez and Cabrera, 2002; Barsó et al. 2003), and by minimal subsidence rates probably related to the transition from the step over structural stage to the double restraining bend stage (Ferrús 1998; Santanach et al. 2005; 13B in Figure 1c).

The deposits of sequence 13 commonly range between 15 and 30 meters (m) in thickness, whereas these deposits attain their maximum thicknesses (around 60 meters) in the eastern subbasin. Figure 2b shows a map of the lower interval (13A), which is characterized by the accumulation of up to 16 m thick coal seam in the inner basin zones. This seam interfingers with the alluvial fan deposits, which were mainly restricted to the eastern marginal zone of the basin. Figure 2c shows a map of the upper interval (13B), which overlies interval 13A. During the 13B interval, the coarser-grained facies impinged into the

inner basin zones, causing the consequent coal facies disappearance (Cabrera et al. 1996, Ferrús 1998).

In the eastern basin area, four zones can be defined based on the overall distribution of the sand and sandy facies in sequence 13 (Figures 2b and 2c). The northern and southern marginal zones (a and b, respectively, in Figure 2a) were affected by minor transverse alluvial fan systems. The marginal eastern (MBZ – Marginal Basin Zone) and inner central basin zones (IBZ – Inner Basin Zone; Figure 2a) were affected by the deposition of a larger axially spread alluvial fan (up to 2.5 km in length and 1.3 km in width, Figures 2b and 2c). The major, laterally extensive sand bodies of this axial alluvial fan that accumulated in the MBZ and IBZ are the main objective of this study.

## **Data sets of the axial alluvial fan successions studied**

More than 675 wells, amounting to approximately 10,000 m of core description, were available for the study of sequence 13. Of these wells, 151 are located in IBZ and 56 in MBZ. Wells were placed along a nearly regular square grid spaced at about 105 m (Figure 2a). The available core descriptions resolve beds thicker than 0.15 m.

### ***Facies description and interpretation***

More than 30 individual facies were differentiated in the original descriptions according to their lithological (textural) and sedimentological characteristics. These individual facies were assembled herein into five major facies: 1) sand (including muddy sands and very minor sandy fine-grained gravels), 2) sandy mudstone, 3) mudstone, 4) coaly mudstone, and 5) coal. Each major facies has a significant occurrence in the studied sequence, and assembles those individual facies that were deposited in closely related

paleoenvironments and share similar sedimentological and petrophysical properties. Apart from the core descriptions, the open pit mining trenches in the basin fill yielded additional evidence of the main geometric and depositional characteristics of these five major facies, as shown in [Figure 3](#).

### **Sand facies**

Sand facies are mainly composed of quartzarenites with minor feldspar grains, and ranges from light coloured whitish-greenish to grey. Clay minerals in the matrix are mainly kaolinite, aluminous smectite and minor illite ([Sáez et al. 2003](#)). The deposits of this facies organize according to two major geometries, with changing sedimentological characteristics ([Ferrús 1998](#)): a) laterally extensive sand bodies, and b) lenticular ribbon sand bodies.

a) The laterally extensive (several hundred meters) sand bodies may be single or multi-episodic and range from a few decimetres up to several meters in thickness. These sand bodies include poorly-sorted (even muddy) coarse, massive sand beds; however, well-sorted, medium to fine and massive to cross-stratified-laminated sands also are present ([Figure 3a](#)). Their changing depositional characteristics indicate that these sand bodies resulted from diverse depositional processes. The widespread coarser, poorly mature in texture sands can be interpreted as relatively proximal sheet flow deposits. The finer, more mature sands would be either the results of sheet flow deposits or flashy channel to overbank deposits formed in braided fluvial fringes, which would have developed mainly in the medial to medial-distal alluvial fan zones. These laterally extensive sand bodies accumulated from relatively proximal to medial alluvial fan zones, attaining only a minor development in the distal zones. As a consequence, these sand bodies are especially widespread in the MBZ and attain lesser development in the IBZ.

b) The lenticular ribbon sand bodies (Friend 1983; Miall 1996) consist of moderately to well-sorted coarse to fine-grained, cross-stratified to laminated sands (Figure 3b). These bodies can also be single to multiepisodic, range from a few decimeters up to a few meters in thickness, and are very continuous along the paleocurrent trends (at least several hundred meters); however, they show a very limited lateral extension across their transverse section (few tens of meters), as observed in the open pit mining trenches (Figure 3b). Most of these ribbon sands were deposited in terminal distributive fluvial plains developed ahead from the narrow braided-channel fringes characteristic of the medial alluvial fan zones. Thus, they are especially widespread in the IBZ and scarcer in the MBZ.

### **Sandy mudstone facies**

The sandy mudstone facies is light colored (green, grey) and make up mostly massive beds. Sand grains are made up mainly of quartz and minor feldspar, whereas clay minerals (kaolinite, aluminous smectite, and illite) occur in the mud grade (Sáez et al. 2003). This facies makes up laterally extensive, thick and multiepisodic bodies that were mostly deposited on the proximal to medial alluvial fan zones of the MBZ, where the core data show its close vertical and lateral relations with the sand facies. Thinner sandy mudstones bodies often overly and interfinger with the mudstone facies in the IBZ successions, recording the progradational alluvial fan stages (13B). The textural and sedimentological characteristics of the sandy mudstone facies indicate that this facies was deposited mainly by sheet flows spreading from the proximal to the medial alluvial fan zones. In the distal medial to distal alluvial fan successions, this facies is also laterally related with channelized braided sand facies and would record poorly sorted overbank, flashyflood deposits.

### **Mudstone facies**

The siliciclastic mudstone facies range from light colored (green, grey) to light brown and is mainly massive (Figure 3c). It is composed mainly by clay minerals (kaolinite, aluminous smectite, and illite) and minor quartz and feldspars (Sáez et al. 2003). Siderite-bearing mudstone beds have been observed in the lower part of sequence 13, in the transition from the underlying coal seam. This facies is dominant in the IBZ successions that record the progradational alluvial fan stages (13B), and was deposited on distal-marginal mud flats, which graded from the medial-distal alluvial fan zones and surrounded the marsh-swamp environments.

### **Coaly mudstone facies**

Coaly mudstone is massive and characterized by dark grayish to brown colors and high terrestrial organic matter content. The mudstone is made up mainly by clay minerals (early diagenetic kaolinite and subordinated illite; Sáez et al. 2003). This facies is widespread in the IBZ successions recording the retrogradational alluvial fan stage (13A) and developed in transitional environments between distal mud flats and the outer margins of the marsh swamp, peat-forming zones.

### **Coal facies**

The coal facies includes a variety of huminite dominated dark brown coal (Figure 3d), liptinite-rich pale brown coal derived from the accumulation of highly degraded aquatic and marsh plant remains, and xyloid brown coal recording the accumulation of wood remnants. These organic rich facies have been described elsewhere (Cabrera et al. 1992 and 1995; Hagemann et al. 1997; Huerta et al. 1997a; Huerta 1998 and 2001; Falivene et al. in press a), and were deposited in marsh-swamp zones where a variety of terrestrial and aquatic plant communities developed (Cavagnetto 2002; Martin-Closas 2003). These environments

developed in the IBZ, at the foot of the terminal alluvial fan zones, and during the retrogradational alluvial fan stage.

### ***Sedimentological-paleoenvironmental general interpretation***

The sedimentological features of the alluvial fan facies, and their relations with the organic rich facies observed in the core descriptions and the open-pit mining trenches (Ferrús 1998; Sáez et al. 2003), indicate depositional zonation from proximal-medial to distal alluvial fan facies, and then to the marsh-swamp, organic-rich facies (the latter only well developed in the 13A interval). Highly sediment concentrated sheet flows and mudflows were probably the main depositional processes on the proximal alluvial fan zones neighboring the fan apex, although the available well data set does not cover entirely these zones. Diluted sheet flows and braided fluvial floods, which gave rise to water-laid laterally extensive to lenticular sand deposits, were more significant in the medial to distal zones, where terminal distributive channel-fringes and mud-flat deposition was dominated by fine and very fine-grained silicilastics. In summary, the axial alluvial fan in sequence 13 can be described as a mudflow and sheet flow, fine-grain dominated fan (Stanistreet and McCarthy 1993; Blair and MacPherson 1994; Miall 1996).

### ***The aquifer system***

Alluvial fan sand-related aquifers in the sequence 13 are multiple-aquifer systems made up of discontinuous sand and very minor gravel bodies embedded in a major matrix of low-permeability facies. Aquitard hydrofacies make up very laterally continuous units (from 200-300 meters up to a 5-10 kilometers), with thicknesses ranging from a 3-4 centimeters up to 5-10 meters, and very low permeabilities (from 0.04 mD to 0.3 mD). This hydrofacies is composed of coal, coaly mudstone, mudstone, and sandy mudstone facies; the latter being the most common aquitard facies. Aquifer hydrofacies is made up by sand facies, is not so

laterally persistent, and is characterized by higher permeability values (from 3 mD to 80 mD). Ribbon sand bodies would show the highest permeability values in the aquifer hydrofacies, whereas the laterally extensive sand bodies would have lower permeability values.

## **Geostatistical reconstruction of the laterally extensive sand bodies**

The large amount and high density of core data allowed the application of a deterministic geostatistical approach for the reconstruction of the 3D distribution of facies in the sequence 13 (Johnson and Dreiss 1989; Ritzi et al. 1995; Falivene et al. in press b). The analysis of the axial alluvial fan unit in the mid-distal and distal zones also benefited from direct observations of the open-pit mining trenches (Figure 3e). The combination of both subsurface and outcrop data enabled a more accurate characterization of the major features of the depositional facies assemblages. Core descriptions are the basis for the geostatistical reconstruction of IBZ and MBZ, with especial focus on the laterally extensive sand bodies developed in the proximal and mid-distal axial alluvial fan successions. The most apical-proximal part of the fan was not included in the model given the absence of well data (Figure 2a).

### ***Grid construction***

The successions gently dip in sequence 13, which was deposited during a relatively quiescent tectonic stage and is affected only by very minor thrusting in the northern basin margin (Figure 1c), causing no significant perturbation to the axial alluvial fan (Figures 2b and 2c) (Ferrús 1998). Therefore, and for simplicity, no faults were considered in the model.

Three surfaces were reconstructed from the triangulation of correlated well data, i.e. the base of interval 13A, the boundary between intervals 13A and 13B, and the top of interval

13B. In order to perform the facies reconstruction, a 3D stratigraphic grid was assigned to sequence 13. Two sub-grids, constrained by the reconstructed surfaces, were defined inside the main grid to reconstruct facies in both intervals independently.

Paleomagnetic studies confirm that the reconstructed surfaces are isochronous or nearly isochronous (Huerta et al. 1997b), and, therefore, correspond to paleodepositional surfaces. To provide a reasonable framework for maximum lateral continuity surfaces, a proportional correlation style was used (Jones 1988, Falivene et al. in press b), with the separation between the layers being proportional to the separation between the top and bottom surfaces for each interval, as depicted in Figure 4. Twenty-eight and 76 layers were used for intervals 13A and 13B, respectively; hence, the mean cell thickness was 0.25 m (ranging from 0 to approximately 0.7 m). Horizontal grid spacing was 25 m. The grid spacing enabled the capture, in detail most of the sedimentary bodies recognized in the wells. The total number of cells within IBZ and MBZ was in the order of 500,000.

The facies logs were up-scaled to the size of grid cells by assigning the most abundant logged facies to each cell (Falivene et al. in press b). In total, over 5,300 cells for interval 13A and approximately 14,000 for 13B were intersected by wells in IBZ and MBZ.

### ***Interpolation algorithm***

Facies reconstruction was carried out using a deterministic geostatistical algorithm. The Markov analysis (e.g. Gingerich 1969) was used as a quantitative tool to determine whether facies transitions should be treated either continuously or categorically. The results obtained suggested that a categorical approach was the most suitable, and, therefore, indicator kriging (IK) was chosen as the interpolation algorithm (Journel 1983; Deutsch and Journel 1992). This deterministic algorithm does not impose any order relations on the facies. IK for categorical variables is based on the decomposition of the categories into several binary

variables, one for each category (Deutsch and Journel 1992). In this case, each category corresponds to a different facies. Each binary variable is set to one whether the related facies occurs, and to zero if it does not. Subsequently, interpolation using ordinary kriging (Matheron 1963; Cressie 1990) is carried out for all the new variables. The results for every category range from 1 (full probability) to 0 (null probability); Figure 5 shows the probability of sand facies occurrence in three sections across the axial alluvial fan. At the end, the category with the highest probability is assigned to each cell.

### ***Variogram estimation***

IK requires estimation of variograms for each category. Starting with the up-scaled facies logs, experimental variogram estimation, theoretical model fitting, and facies interpolation were undertaken using gOcad® (by EARTH DECISION, Mallet 1992). A new coordinate system was defined with the  $z$  dimension transformed into a parametric dimension using the grid cell indices. In this new system, the horizontal planes represent the best approximation to the paleodepositional surfaces (i.e. where the sedimentary bodies should display most lateral continuity).

Variogram analysis was carried out only for well data located in IBZ and MBZ (Figure 2a), where the reconstruction was focused. This analysis led to the definition of horizontal and vertical ranges for each facies. Variogram parameters and variogram curves for sand facies are presented in Table 1 and Figure 6, respectively. As expected, continuity in the paleodepositional plane is larger than in the perpendicular direction. Indicator horizontal variograms for sand facies both anisotropic (major axis elongated along the paleocurrent direction) and isotropic have been described in other alluvial fans (i.e. Johnson 1995). In the alluvial fan successions examined, differences in horizontal experimental variograms along

different azimuths are not significant (Figure 6), and, thus, the theoretical variogram models were fitted with horizontal isotropic ranges.

Some facies (coal in interval 13A, and mudstone and sandy mudstone in interval 13B) show zonal anisotropy in the experimental variograms related to trends in their spatial distribution (Table 1) (Gringarten and Deutsch 2001). This effect was not modeled when fitting the theoretical variogram models, yielding an underestimation of the corresponding ranges. However, such relatively small underestimations do not have any marked effect on the resultant body dimensions when applying IK to regularly distributed and high-density data.

### ***Suitability of data to describe the sand bodies***

IK was used as a tool to achieve a 3D correlation and interpolation of facies described in a large number of wells. Nevertheless, geostatistical interpolation techniques for automatic facies reconstruction should be applied with caution. For bodies with lateral dimensions smaller than well spacing, interpolation would yield unrealistically extensive bodies with no geological sense. In the alluvial fan successions of sequence 13, various lines of evidence suggest that at least some of the sand bodies can be confidently correlated between adjacent wells:

a) As stated above (see [Facies description and interpretation section](#)), the sedimentological analysis of the information from the open-pit mining trenches confirms the presence of some laterally extensive sand bodies, whose lengths exceed 105 m (well spacing).

b) The continuity shown by the horizontal experimental variograms for sand facies at small lags (Figure 6) and the resulting ranges (Table 1) suggest that at least some sand bodies would exhibit lengths exceeding 105 m. It is important to note herein that sand facies groups

bodies with two types of depositional geometries (see [Facies description and interpretation section](#)): the laterally extensive sand bodies, which are responsible for the continuity shown by experimental variograms; and the lenticular ribbon sand bodies, which tend to inflate variogram values and obscure any evidence of correlation due to their small size compared to well spacing. [Ritzi \(2000\)](#) and [Guardiola-Albert and Gómez-Hernández \(2001\)](#) report a quantitative relation among variogram range, proportions, and mean body lengths. Based on this relation, the obtained ranges would lead to mean body lengths of approximately 280 m for sand bodies in interval 13A, and 140 m for sand bodies in interval 13B, when using Sequential Indicator Simulation (SIS, i.e. the simulation form of IK; [Deutsch and Journel 1992](#)). These mean lengths range between one and two well spacings, and, therefore, the sand bodies are defined, on average, by 1 to 3 data points in each of the two horizontal directions.

c) Mean sizes of sand bodies (i.e. volumes), obtained using conditioned SIS varying variogram ranges, were compared with those from the IK facies reconstruction, in order to test the hypothesis that the data spacing is sufficiently small to allow deterministic correlation of the wells. In theory, when the variogram range increases, and the proportions are kept constant, the mean dimensions of sand bodies should also increase ([Carle and Fogg 1996](#); [Ritzi 2000](#); [Guardiola-Albert and Gómez-Hernández 2001](#)). [Figure 7](#) shows the mean size of sand bodies derived from SIS with several horizontal ranges, and the mean size of sand bodies from the IK reconstruction with the experimentally fitted ranges ([Figure 6](#)). As the horizontal range increases, the mean sizes from SIS tend to stabilize at a value because of the control exerted by the densely spaced conditioning well data (i.e. the high-density data do not allow simulating larger sand bodies). Moreover, the mean size at which the sand bodies derived from SIS stabilize is close to the one resulting from IK, and the stabilization is practically achieved for ranges comparable to the ones deduced from the available core data.

This result suggests that well data can be deterministically correlated, and are sufficient to reconstruct at least the laterally extensive sand bodies accumulated in the studied sequence.

## **Results and discussion: Characterization of the sand bodies**

### ***General facies distribution***

Figure 8 shows the 3D reconstruction of the laterally extensive sand bodies in the axial alluvial fan successions located within MBZ and IBZ, as provided by the interpolation results derived using IK (see [Geostatistical reconstruction of the laterally extensive sand bodies](#) section).

During interval 13A, sedimentation was dominated by coal accumulation in most of IBZ, and the coarser grained facies of the proximal and middle alluvial fan environments remained very restricted to MBZ ([Figure 2b](#), [Table 2](#)). On the other hand, during the subsequent progradational evolutionary stage (interval 13B), sandy mudstones and sands dominated in MBZ, whereas mudstones and sandy mudstones spread in IBZ ([Figure 2c](#), [Table 2](#)). This evolution was paralleled by the thicker accumulation and concentration of sand facies in MBZ and with their significant, albeit lower, proportions in the IBZ during both intervals.

### ***Inferred shape and dimensions of the sand bodies***

Laterally extensive sand bodies within IBZ and MBZ were individualized using face connection between grid cells (following the sense of [Deutsch 1998](#)), as shown in [Figures 8b and 8c](#). These bodies were characterized by means of summary statistics on their dimensions, presented in [Figures 9 and 10](#): a) volume ([Figure 9](#)), b) mean thickness ([Figure 10a](#)), and

maximum equivalent diameter (Figure 10b). Maximum equivalent diameter corresponds to the diameter of a circle with the same maximum area of the selected sand body; this simplification provides us with an approximation to their maximum length, parallel, and perpendicular to the paleocurrent. Only the results for the 37 laterally extensive sand bodies intercepted by at least two wells are presented herein, and a number of characteristics from these bodies must be summarized:

1) These laterally extensive sand bodies include more than 95% of the sand present in the reconstructed axial alluvial fan.

2) Most of these sand bodies show irregular boundaries, and although some of them appear in the reconstruction as elliptical, this apparent simplicity is because the data are not sufficiently dense to capture shapes that are more detailed.

3) Most of the laterally extensive sand bodies show relatively small mean thicknesses (up to 2 m), and small maximum equivalent diameters (from 100 to 300 m). Some bodies are thicker (from 3 to 5 m, and exceptionally up to 11 m), and larger (maximum equivalent diameter ranging from 300 to 800-1000 m), because of intense stacking and amalgamation. As shown in Figure 11, thickening is usually paralleled by an increase in the maximum equivalent diameter.

4) The most significant accumulations of sand facies are recorded in MBZ, both in intervals 13A and 13B. The largest sand bodies tend to concentrate there, although some exceptions occur in IBZ during interval 13B (Figures 9 and 10). In MBZ, most of the sand volume corresponds to a few, very large, multiepisodic bodies. In the more proximal parts of the axial alluvial fan (eastern part of MBZ), laterally and vertically stacked sand deposits were dominant during interval 13B because of the increasing proportion of sand. The largest sand body ( “ $\alpha$ ” body) occurs there, characterized by a maximum equivalent diameter of

more than 1,000 m, a mean thickness around 11 m, and accounting for approximately 65% of the sand deposited in the axial alluvial fan during sequence 13 (Figures 8a, c, 9, and 11).

5) By contrast to item 4 above, the sand facies volume accumulated in IBZ is significantly smaller, especially during interval 13A, and during interval 13B, corresponds to a larger number of smaller bodies (Figure 9).

Other sand bodies, which account for the remaining sand volumes deposited in the alluvial fan, also occur in IBZ and MBZ. These correspond to ribbon paleochannel sands, which cannot be mapped with the available data because of their reduced transverse section (see Facies description and interpretation section), in the reconstruction are mainly expressed as isolated pods, and, therefore, their dimensions are not presented herein.

### ***Generation of single to multi-episodic laterally extensive sand bodies***

Both field and well observations, coupled with the results of the 3D reconstruction, enabled the precise description of general depositional features of the alluvial fan facies, and provided a better comprehension of the generation and distribution of the laterally extensive sand bodies. The occurrence in fine-grain alluvial fans of single to multi-episodic, laterally extensive sand bodies depends on the more or less repeated development of water laid and/or winnowed deposits (Galloway and Hobday 1996; Miall 1996). In the MBZ, these deposits were associated with the frequent depositional action of sheet floods, which would have resulted in sheet sands. Moreover, in some cases, subsequent braided stream deposition and/or reworking result in the generation of laterally extensive sand bodies (Galloway and Hobday 1996; Miall 1996, Blair and McPherson 1994; Blair 2003). Some of the laterally extensive sand bodies that developed in the medial to medial-distal alluvial fan zones of the

MBZ might have resulted also from cycles of trench generation, backfilling, and dispersion of shallow braided channel systems (Schumm 1987; DeCelles et al. 1991).

### ***Implications for aquifer modeling and exploitation***

As discussed in the [Suitability of data to describe the sand bodies](#) section, the sampling well grid captures the laterally extensive sand bodies, allowing their satisfactory and reliable reconstruction. Given the densely spaced conditioning data, it would be of little value either to introduce trends in the proportions (see examples in [Journel and Rossi 1989](#), and [Falivene et al. in press a](#)) or use different variograms (i.e. varying ranges or anisotropy directions), for each zone of the axial alluvial fan reconstructed herein. However, variation in facies proportions and variograms along the different alluvial fan zones should be considered when modeling a similar alluvial fan utilizing a stochastic modelling technique with a less closely spaced data set.

The occurrence of unconfined depositional processes, which are typical of the proximal parts of the alluvial fan, and the lateral stacking of sand deposits, would partially overcome the typical elongation tendency of sand bodies along the paleocurrent direction that has been observed in other alluvial fans. These observations (together with uncontrolled small topographic variations or undulations, the presence of non-correlatable lenticular ribbon sand bodies, and curvilinear trends) may also account for the resulting isotropy of the horizontal variogram ranges for sand facies.

The reported parameters ([Figures 911](#)) can be used to define geological scenarios for modeling similar alluvial fan aquifers. These parameters relate to the laterally extensive sand bodies, which account for the majority of sand facies, and, therefore, porosity in fine-grain dominated alluvial fans. For a more complete modeling of similar depositional systems, the lenticular ribbon sand bodies, which are resolved as isolated pods in the provided

reconstruction (Figures 2 and 8), should be also included and realistically reproduced. These bodies are mainly related to the development of fluvial water laid deposits, and often occur in the medial to distal basin zones where a distributive fluvial drainage developed (see [Facies description and interpretation](#) section). It was not possible to provide a reliable reconstruction and quantification of these bodies because the well grid does not capture them. However, outcrop observations indicate that lenticular ribbon sand bodies can extend considerably along paleocurrent direction and have the potential to connect several extensive sheet sand bodies. In addition, ribbon sand bodies are typically made up of well-sorted and very permeable material and, thus, may act as preferential pathways for fluid transport.

## **Concluding remarks**

The aquifers composed of fine-grained dominated alluvial fans are characterized by a clear predominance of the aquitard over the aquifer hydrofacies. Thus, aquifer hydrofacies may present a more sparse and unpredictable distribution. The use of indicator kriging applied to a high-density data set enabled reconstruction and interpretation of the hydrofacies structure of a fine-grain dominated alluvial fan. When there is sufficient data density to capture the geological heterogeneity, this method can provide reliable reconstructions of the aquifer-aquitard hydrofacies distribution. A further insight into the heterogeneity of the alluvial system and its origin was obtained through field observation and comparison of the results with the findings of previously described depositional models.

The facies reconstruction enabled us to quantify trends, volumes, mean thickness, maximum area, and maximum equivalent diameter of the laterally more extensive sand bodies. The reconstruction of these bodies resulted in a wide range of dimensions as a function of their changing single or multi-episodic character. This resulted from the

frequency and distribution of dominant depositional processes in the diverse alluvial fan and basin zones. Both frequency and distribution varied during the overall progradational evolution of the alluvial system. The successive retractive and expansive situations of the alluvial fan system were contrasted in accordance with the quantified characteristics of the sand bodies. In the retracted alluvial fan interval (13A), fewer laterally extensive sand bodies occur and these were deposited mainly in the eastern marginal basin zone. During the alluvial fan expansive interval (13B), the number of laterally extensive sand bodies increased in the marginal and the inner basin zones. Nevertheless, sand grade concentrated in the marginal basin zones in a few bodies that resulted from intense amalgamation; the largest body amounting to 65% of the sand deposited in the axial alluvial fan during the entire sequence.

The hydrofacies distribution trends and dimensions of the laterally extensive sand bodies can be used as scenarios for input statistical parameters when modeling aquifer/aquitard hydrofacies in similar fine-grained dominated alluvial fans, or when evaluating poorly known alluvial fans considering different geological scenarios. These compilations may help to evaluate and reduce uncertainty in the statistical parameters used for building facies models. Thus, in the facies models themselves, which will provide better predictions of hydraulic parameter distributions, and, therefore, will improve overall alluvial fan aquifer comprehension and exploitation. However, it should be pointed out that the estimated absolute dimensions and sand fractions could change as a function of geological and climatic constraints despite similar overall trends and processes. The manner in which these parameters can be extrapolated to bigger alluvial fans is still a matter of debate and further quantifications of different alluvial fans are warranted.

The characterization of the occurrence probability, geometry, and distribution of the laterally extensive sand deposits provides also a more accurate geological framework in which to carry out further numerical models of groundwater flow and solute transport.

## **Acknowledgements**

This research was carried out in the Geomodels Institute. This institute is sponsored by Generalitat de Catalunya (DURSI) and Instituto Geológico y Minero de España (IGME) and includes the 3D Geological Modelling CER (University of Barcelona). The authors are indebted to ENDESA MINA PUENTES for providing the database, including original core descriptions and permeability measurements. The Department of Geology of the University of Barcelona is also acknowledged for friendly support and field guidance. Financial support from the MCyT-MEC (Proyectos CARES BTE 2001-3650 and MARES CGL 2004-05816-C02-02/BTE) and from the Generalitat de Catalunya (Grup de Recerca de Geodinàmica i Anàlisi de Conques, 2001SGR-000074) is acknowledged. Research by O. Falivene is funded by a MEC pre-doctoral grant from the Spanish Government. Discussions with the colleagues at the gOcad user and research discussion lists and general comments by T.C. Blair are kindly appreciated. F.D. Dominic and O. Fernández carefully revised a preliminary version of the manuscript, which was also improved thanks to the comments by the Associate and the Managing Editors and by two anonymous reviewers.

## **Reference list**

Anderson MP (1989) Hydrogeologic facies models to delineate large-scale spatial trends in glacial and glaciofluvial sediments. *Geological Society of America Bulletin* 101:501-511

- Bacelar J, Alonso M, Kaiser C, Sanchez M, Cabrera L, Sáez A, Santanach P (1988) La Cuenca Terciaria de As Pontes (Galicia): su desarrollo asociado a inflexiones contractivas de una falla direccional (The As Pontes Tertiary basin, development linked to restraining bends in a directional fault). Proceedings of the II Geological meeting of Sapin, Sociedad Geológica de España, 113-121.
- Baltuille JM, Becker-Platen JD, Benda L, Ivanovic Calzaga Y (1992) A contribution to the division of the Neogene in Spain using palynological investigations. Newsletter Stratigraphy 27:41-57
- Barsó D, Cabrera L, Marfil R, Ramos E (2003) Catchment evolution of the continental strike-slip As Pontes basin (Tertiary, NW Spain): constraints from the heavy mineral analysis. Revista de la Sociedad Geológica de España 16:73-89
- Blair TC, MCPerson JG (1994) Alluvial fans and their natural distinction from rivers based on morphology, hydraulic processes, sedimentary processes, and facies assemblages. Journal of Sedimentary Research A64:450-489.
- Blair TC (2003) Features and origin of the giant Cucomungo Canyon alluvial fan, Eureka Valley, California. Geological Society of America Special Paper, 370: Extreme depositional environments: mega end members in geological time: 105-126
- Bryant ID, Flint SS (1993) Quantitative clastic reservoir geological modelling: problems and perspectives. In: Flint SS, Bryant ID (eds) The Geologic Modelling of Hydrocarbon Reservoirs and Outcrop Analogues. Vol 15. Special Publications of the International Association of Sedimentologists, pp 3-20
- Bull WB (1964a) Geomorphology of segmented alluvial-fans in western Fresno County. U.S. Geological Survey Professional Paper 352-E:89-129.
- Bull WB (1964b) Alluvial-fans and Near-Surface Subsidence in western Fresno County. U.S. Geological Survey Professional Paper 437-A:1-71
- Bull WB (1991) Geomorphic responses to Climate Change, New York, Oxford University Press.
- Cabrera L, Hagemann HW, Pickel W, Sáez A (1992) Caracterización Petrológica y Geoquímica Orgánica de los lignitos de la cuenca de As Pontes (La Coruña). Proceedings of the II Geological Meeting of Spain - VIII Geological meeting of Latinoamerica 2: 239-246.
- Cabrera L, Jung W, Kirchner M, Sáez A (1994) Crocodilian and Paleobotanical findings from tertiary lignites of As Pontes Basin (Galicia, NW Spain). Cour. Forsch. Inst. Senckenb. 173:153-165
- Cabrera L, Hagemann HW, Pickel W, Sáez A (1995) The coal-bearing, Cenozoic As Pontes Basin (northwestern Spain): geological influence on coal characteristics. International Journal of Coal Geology 27:201-226.
- Cabrera L, Ferrús B, Sáez A, Santanach P, Bacelar J (1996) Onshore Cenozoic strike-slip basins in NW Spain. In: Friend PF, Dabrio CJ (eds) Tertiary Basins of Spain, the Stratigraphic Record of Crustal Kinematics, pp 247-254

- Campbell C (1998) Postglacial evolution of a fine grained alluvial fan in the northern Great Plains, Canada. *Palaeogeography, Palaeoclimatology, Palaeoecology* 139:233-249
- Carle SF, Fogg GE (1996) Transition probability based indicator geostatistics. *Mathematical Geology* 28:453-476
- Carle SF, Labolle EM, Weissmann GS, Van Brocklin D, Fogg GE (1998) Conditional Simulation of Hydrofacies Architecture: A Transition Probability/Markov Approach. In: Fraser GS, Davis JM (eds) *Hydrogeologic models of sedimentary aquifers. Vol 1: Concepts in Hydrogeology and Environmental Geology*, pp 147-170
- Cavagnetto C (2002) La palynoflore du Bassin d'As Pontes en Galice dans le Nord Ouest de l'Espagne à la limite Rupélien-Chattien (Oligocène). *Palaeontographica. Abteilung B: Paläophytologie* 263:161-204
- Cressie N (1990) The origins of kriging. *Mathematical Geology* 22:239-252
- de Marsily G, Delay F, Teles V, Schafmeister MT (1998) Some current methods to represent the heterogeneity of natural media in hydrogeology. *Hydrogeology Journal* 6:115-130
- de Marsily G, Delay F, Gonçalves J, Renard P, Teles V, Violette S (2005) Dealing with spatial heterogeneity. *Hydrogeology Journal* 13:161-183, DOI 10.1007/s10040-004-0432-3
- DeCelles PG, Gray MB, Ridgway KD, Cole RB, Pivnik DA, Pequera N, Srivastava P (1991) Controls on synorogenic alluvial-fan architecture, Beartooth Conglomerate (Palaeocene), Wyoming and Montana. *Sedimentology* 38:567-590
- Deutsch CV, Journel A (1992) *GSLIB Geostatistical Software Library and user's guide*. Oxford University Press
- Deutsch CV, Hewett TA (1996) Challenges in Reservoir Forecasting. *Mathematical Geology* 28:829-842
- Deutsch CV (1998) Fortran programs for calculating connectivity of three dimensional numerical models and for ranking multiple realizations. *Computers & Geosciences* 24:69-76
- Dreyer T, Falt LM, Hoy T, Knarud R, Steel R, Cuevas JL (1993) Sedimentary architecture of field analogues for reservoir information (SAFARI): a case study of the fluvial Escanilla Formation, Spanish Pyrenees. In: Flint SS, Bryant ID (eds) *The Geological Modelling of Hydrocarbon Reservoirs and Outcrop Analogues. Vol 15. IAS Special Publication*, 57-80.
- Falivene O, Arbués P, Howell J, Muñoz JA, Fernández O, Marzo M. (2006a) Hierarchical geocellular facies modelling of a turbidite reservoir analogue from the Eocene of the Ainsa Basin, NE Spain. *Marine and Petroleum Geology* 23:679-701.

- Falivene O, Arbués P, Gardiner AR, Pickup GE, Muñoz JA, Cabrera L (2006b) Best-practice stochastic facies modeling from a channel-fill turbidite sandstone analog (the "Quarry Outcrop", Eocene Ainsa Basin, NE Spain). *American Association of Petroleum Geologists Bulletin* 90:1003-1029.
- Falivene O, Cabrera L, Saez A (in press a) Optimum and robust 3D facies interpolation strategies in a heterogeneous coal zone (Tertiary As Pontes basin, NW Spain). *International Journal of Coal Geology*.
- Falivene O, Cabrera L, Muñoz JA, Arbués P, Fernández O, Sáez A (in press b) Statistical grid-based facies reconstruction and modelling of sedimentary bodies. Alluvial-palustrine and turbiditic selected examples. *Geologica Acta*
- Falkner A, Fielding C (1993) Quantitative facies analysis of coal-bearing sequences in the Bowen Basin, Australia: applications to reservoir description. In: Flint, SS, Bryant, ID (eds) *The Geologic Modelling of Hydrocarbon Reservoirs and Outcrop Analogues*. Vol 15. IAS Special Publication, pp. 81-98.
- Ferrús B (1998) Análisis de cuenca y relaciones tectónica-sedimentación en la cuenca de As Pontes (Galicia) (Basin analysis and tecto-sedimentary relationships in the As Pontes basin). PhD. Thesis. Barcelona University
- Fogg GE, Noyes CD, Carle SF (1998) Geologically-based model of heterogeneous hydraulic conductivity in an alluvial setting. *Hydrogeology Journal* 6:131-143
- Fraser GS, Suttner L (1986) *Alluvial fans & Fan Deltas. A guide to exploration for oil and Gas*, Boston
- Friend PF (1983) Towards the field classification of alluvial architecture or sequence. In: Collinson JD, Lewin J (eds) *Modern and ancient fluvial systems*. Vol 6. IAS Social Publication, pp 345-354
- Galloway WE, Hobday DK (1996) *Terrigenous Clastic Depositional Systems: Application to Fossil Fuel and Groundwater Resources*. Springer
- Gingerich PD (1969) Markov Analysis of cyclic alluvial sediments. *Journal of Sedimentary Petrology* 39:330-332
- Gómez-Hernández JJ, Deutsch CV (1999) Foreword to Special Issue: Modeling Subsurface Flow. *Mathematical Geology* 31:747-748
- Gringarten E, Deutsch CV (2001) Variogram interpretation and modeling. *Mathematical Geology* 33:507-535
- Guardiola-Albert C, Gómez-Hernández J (2001) Average length of objects generated by a binary random function: discretization effects and relation with the variogram parameters. *Proceedings of the geoENV III*. Avignon (France)
- Hagemann HW, Pickel W, Cabrera L, Sáez A (1997) Tertiary lignites of the As Pontes (NW Spain) - An example for composition of bright coal layers and its implications for formation. *Proceedings of the 9th International Conference on Coal Science* 1: 31-34

- Haldorsen HH, Damsleth E (1990) Stochastic Modeling. *Journal of Petroleum Geology* 42:404-412
- Harvey AM (1989) The occurrence and role of arid zone alluvial fans. In: Thomas DSG (ed) *Arid Zone Geomorphology*. Halsted Press, New York, pp 136-158
- Hornung J, Aigner T (1999) Reservoir and aquifer characterization of fluvial architectural elements: Stubensandstein, Upper Triassic, southwest Germany. *Sedimentary Geology* 129:215-280
- Huerta A, Querol X, Sáez A, Cabrera L (1997a) Mineralogy and Geochemistry of the As Pontes lignites (NW Spain): Relation with paleohydrological basin evolution. In: *Migration and Interaction in Sedimentary basins and Orogenic Belts. GEOFLUIDS II'97. Contributions to the Second International Conference on Fluid Evolution*. Geological Society Special Publication, pp 370-373
- Huerta A, Parés JM, Cabrera L, Ferrús B, Sáez A (1997b) Magnetocronología de las sucesiones cenozoicas de la cuenca de As Pontes (La Coruña, Noroeste de España). *Acta Geológica Hispánica* 32:127-145
- Huerta A (1998) Petrografía, Mineralogía y Geoquímica de los lignitos de la cuenca Oligo-Miocena de As Pontes (A Coruña): Control geológico sobre la calidad del carbon. PhD. Thesis. Barcelona University.
- Huerta A (2001) Resumen de tesis Doctoral: Caracterización mineralógica y geoquímica de los lignitos de la cuenca Terciaria de As Pontes (Provincia de La Coruña). *Acta Geológica Hispánica* 36, 183-186
- Johnson JM, Dreiss SJ (1989) Hydrostratigraphic interpretation using indicator geostatistics. *Water Resources Research* 25:2501-2510
- Johnson NM (1995) Characterization of alluvial hydrostratigraphy with indicator semivariograms. *Water Resources Research* 31:3217-3227
- Jones TA (1988) Geostatistical Models with Stratigraphic Control - Short Note. *Computers and Geosciences* 14:135-138
- Journel AG (1983) Nonparametric Estimation of Spatial Distributions. *Mathematical Geology* 15:445-468
- Journel AG, Rossi M (1989) When do we need a trend in kriging? *Mathematical Geology* 21:715-739
- Jussel P, Stauffer F, Dracos T (1994) Transport modelling in heterogeneous aquifers 1: Statistical description and numerical generation of gravel deposits. *Water Resources Research* 30:1803-1817
- Koltermann CE, Gorelick SM (1996) Heterogeneity in sedimentary deposits: A review of structure-imitating, process-imitating, and descriptive approaches. *Water Resources Research* 32:2617-2658
- Kupfersberger H, Deutsch CV (1999) Methodology for Integrating Analog Geologic Data in 3-D Variogram Modeling. *American Association of Petroleum Geologists Bulletin* 83:1262-1278

- Legget RF, Brown RJE, Johnson GH (1966) Alluvial fan formation near Alavik, Northwest Territories, Canada. *Geological Society of America Bulletin* 77:15-30
- Mallet JL (1992) Gocad: a computer aided design program for geological applications. In: *Three-dimensional modeling with geoscientific information systems*. Kluwer Academic Publishers, pp 123-141
- Manera A, Barrera JL, Cabal JM, Bacelar J (1979) Aspectos geológicos de la cuenca terciaria de Puentes de García Rodríguez (La Coruña). *Boletín Geológico y Minero* 95:542-561
- Martín-Closas C (2003) The fossil record and evolution of freshwater plants: A review. *Geologica Acta*. 1:315-338
- Matheron G (1963) Principles of geostatistics. *Economic Geology* 58:1246-1266
- Médus J (1995a) Contribution palynologique à la connaissance de la flore et de végétation néogène de l'ouest de l'Espagne. Étude des sédiments récents de Galice.. PhD. Thesis. Univ. Montpellier
- Médus J (1995b) L'évolution biostratigraphique d'une lagune néogène de Galice (Espagne). *Pollen et spores* 7:381-391
- Menéndez Amor J (1975) Análisis paleobotánico de algunas muestras de lignitos procedentes de Puentes de García Rodríguez (La Coruña). *Boletín de la Real Sociedad Española de Historia Natural (Geología)* 73:121-124
- Miall AD (1996) *The Geology of Fluvial Deposits*. Springer
- Nakayama K (1996) Depositional processes for fluvial sediments in an intra-arc basin: an example from the upper Cenozoic Tokai Group in Japan. *Sedimentary Geology* 101:193-211
- Nakayama K (1999) Sand- and mud-dominated alluvial-fan deposits of the Miocene Seto Porcelain Clay Formation, Japan. In: Smith ND, Rogers J (eds) *Spec. Pub. Int.Ass. Sediment* , 28: *Fluvial Sedimentology VI*. Blackwell Science, London., pp 393 -407
- Nemec W, Steel RJ (eds) (1988) *Fan Deltas: Sedimentology and Tectonic settings*, Glasgow
- Rachocki AH, Church M (eds) (1990) *Alluvial fans: A Field Approach.*, New York
- Ritzi (1995) Hydrofacies distribution and correlation in the Miami Valley aquifer system. *Water Resources Research* 31:3271-3281
- Ritzi RW (2000) Behaviour of indicator variograms and transition probabilities in relation to the variance in lengths of hydrofacies. *Water Resources Research* 36:3375-3381
- Robinson JW, McCabe PJ (1997) Sandstone-Body and Shale-Body Dimensions in a Braided Fluvial System: Salt Wash Sandstone Member (Morrison Formation), Garfield County, Utah. *American Association of Petroleum Geologists Bulletin* 81:1267-1291.

- Sáez A, Cabrera L (2002) Sedimentological and paleohydrological responses to tectonics and climate in a small, closed, lacustrine system: Oligocene As Pontes Basin (Spain). *Sedimentology* 49:1073-1094
- Sáez A, Inglès M, Cabrera L, de las Heras A (2003) Tectonic-palaeoenvironmental forcing of clay-mineral assemblages in nonmarine settings: the Oligocene-Miocene As Pontes Basin (Spain). *Sedimentary Geology* 159:305-324
- Santanach P, Ferrús B, Cabrera L, Saez A (2005). Origin of a restraining bend in an evolving strike-slip system: The Cenozoic As Pontes basin (NW Spain). *Geologica Acta* 3:225-239
- Santanach P, Baltuille JM, Cabrera L, Monge C, Sáez A, Vidal-Romani JR (1988) Cuencas terciarias gallegas relacionadas con corredores de fallas direccionales. Paper presented at II Congreso Geológico de España. Granada
- Schumm (1987) *Experimental fluvial geomorphology*, New York, Wiley
- Stanistreet IG, McCarthy TS (1993) The Okavango fan and the classification of subaerial fans. *Sedimentary Geology* 85:114-133
- Tye RS (2004) *Geomorphology: An approach to determining subsurface reservoir dimensions*. American Association of Petroleum Geologists Bulletin 88:1123-1147
- Webb EK, Davis JM (1998) Simulation of the spatial heterogeneity of geologic properties: an overview. In: Fraser GS, Davis JM (eds) *Hydrogeologic models of sedimentary aquifers*. Vol 1: Concepts in Hydrogeology and Environmental Geology, pp 1-24
- Weissman GS, Fogg GE (1999) Multi-scale alluvial fan heterogeneity modeled with transition probability geostatistics in a sequence stratigraphic framework. *Journal of Hydrology* 226:48-65
- Weissman SG, Carle SF, Fogg GE (1999) Three-dimensional hydrofacies modeling based on soil surveys and transition probability geostatistics. *Water Resources Research* 35:1761-1770
- Weissman GS, Yong Z, Fogg GE, Blake RG, Noyes CD, Maley M (2002) Modeling alluvial fan aquifer heterogeneity at multiple scales through stratigraphic assessment. Paper presented at Bridging the gap between measurement and modeling in heterogeneous media. Proceedings of the International Groundwater Symposium, Lawrence Berkeley National Laboratory. Berkeley, California, March, 25-28

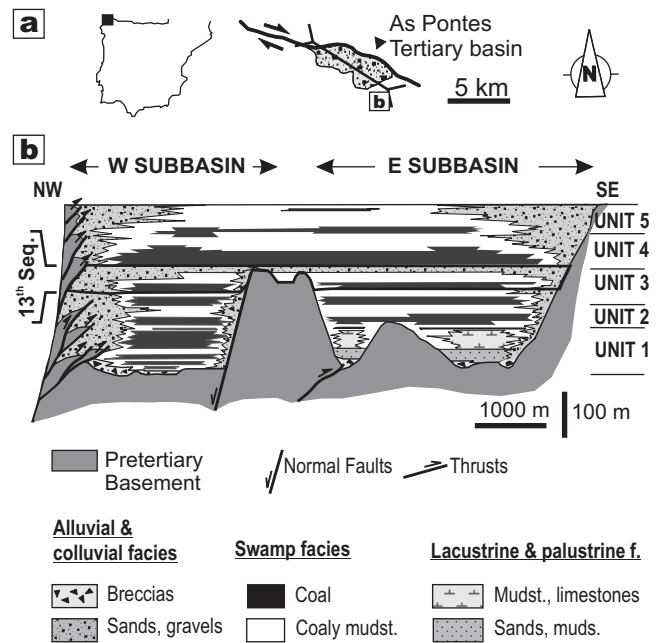


**Figure 1. (a)** Regional geological setting of the As Pontes basin. The Variscan basement consists of Precambrian and Early Paleozoic metamorphic rocks. This basement was affected by the alpine deformation of the northern Iberian margin in the western end of the Pyrenean orogen. **(b)** Longitudinal sketch of the basin showing the main stratigraphic units, sedimentary facies and basement structures (see location on 1a). Notice the stratigraphic position of the 13<sup>th</sup> sequence.

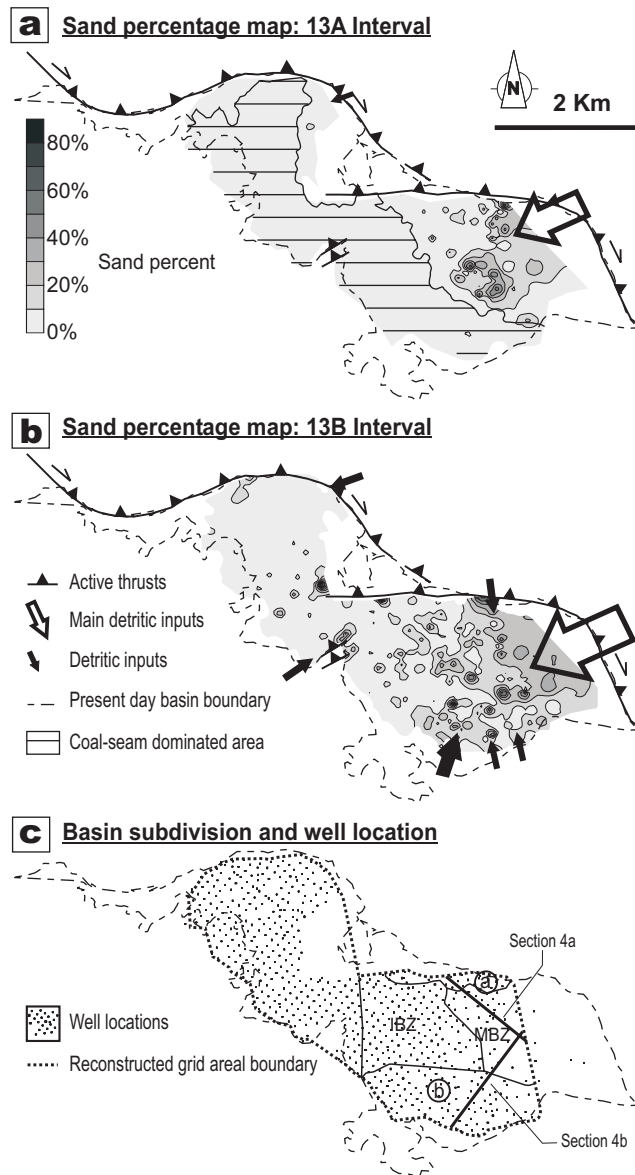


**Figure 2 (a, b)** Sand percentage maps for the intervals A and B in the 13<sup>th</sup> sequence. Arrows show the main alluvial feeding points of coarse-grained facies. The largest ones correspond to the axial alluvial fan. Active structures during the sedimentation of the 13<sup>th</sup> sequence are based on Ferrús (1998). The coal-seam dominated area in the 13A interval is also shown. The boundary encloses the area with coal percentage higher than 60%. **(c)** Well distribution, note regularly spacing, and subdivision of the basin area according to sand deposition patterns: a) alluvial fans attached to the northern, tectonically active margin; b) alluvial fans fed from the southern passive margin; MBZ) marginal basin zones where proximal to middle-proximal axial alluvial fan facies dominated; IBZ) inner basin zones with major development of middle to distal axial alluvial fan facies. Position of cross-sections in Fig. 4 is also shown.

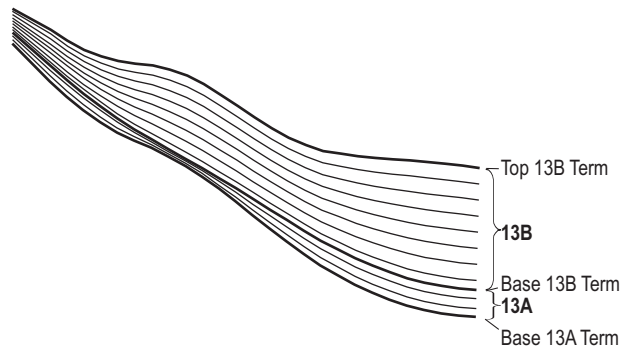


**Figure 3.** Detail of a vertical cross-section showing proportional layering in the two reconstructed sub-grids, note that not only one tenth of the grid layers is shown. Proportional layering is used to model units with wedge out geometries.

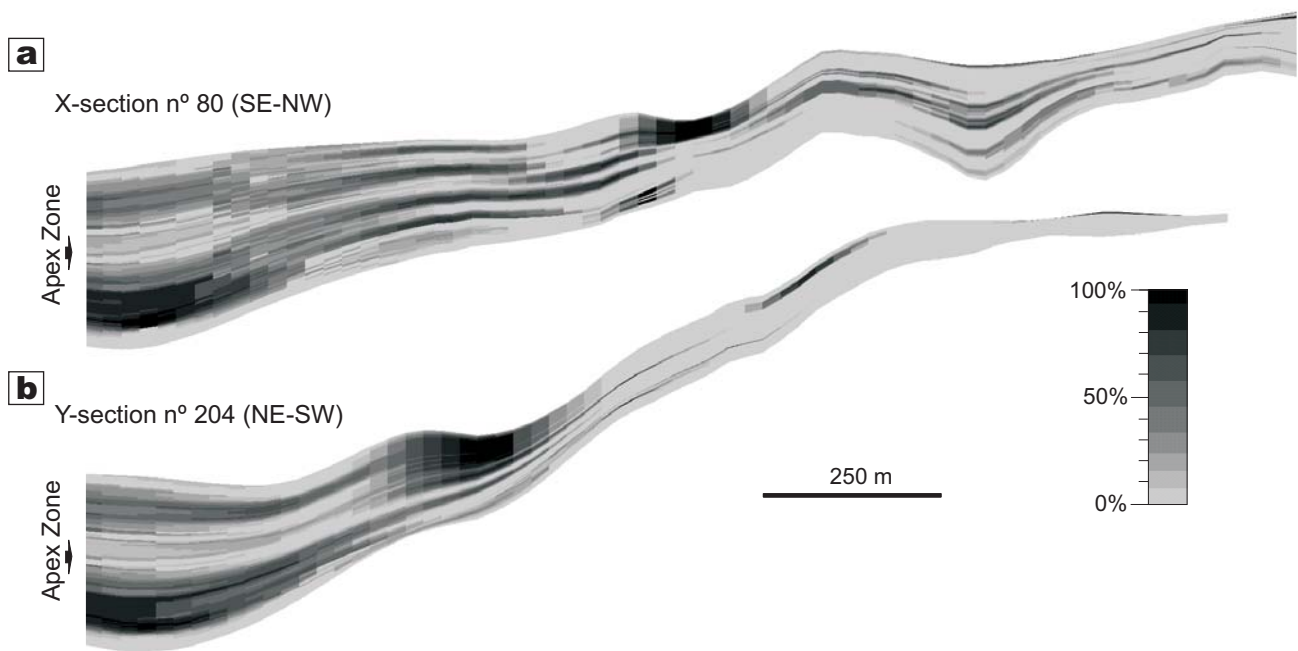


**Figure 4 (a, b)** Cross-sections across the axial alluvial fan; showing probability of relatively high permeability sand hydrofacies occurrence resulting from the interpolation of the indicator variable. Location of cross sections shown in Fig. 2c. Compare with the facies model and the sand-dominated bodies identified in Fig 7b, where the same cross-sections are shown. Vertical exaggeration is x3

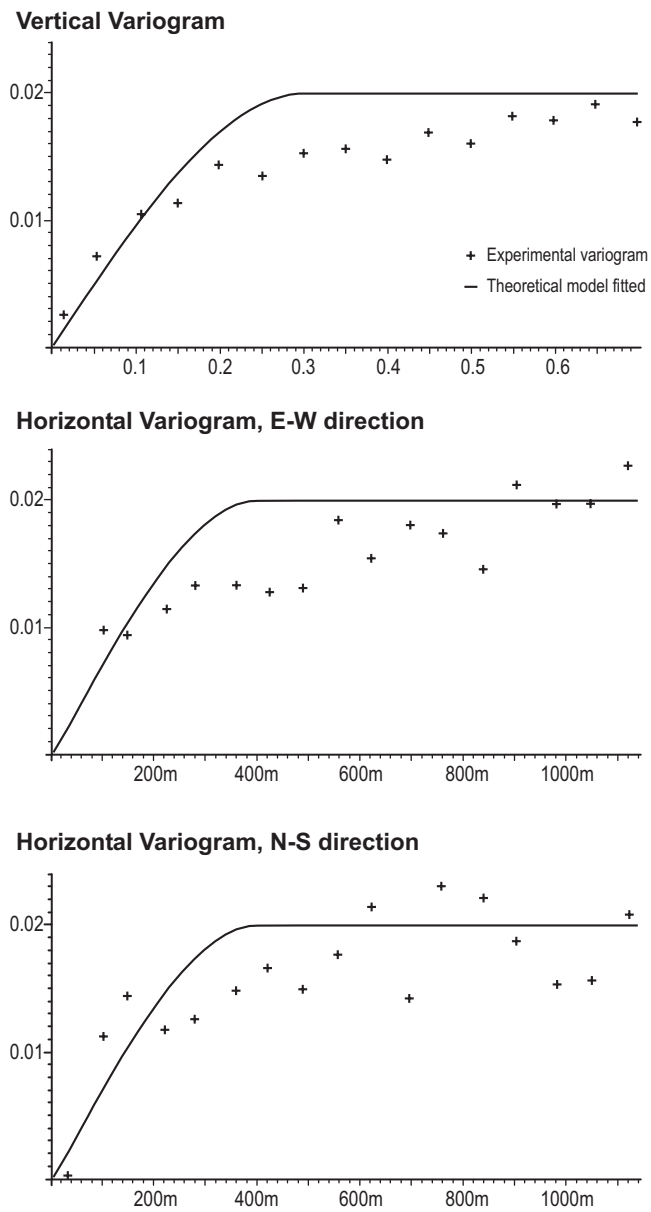


**Figure 5.** Indicator variograms for sand facies at 13A Term. Experimental variograms are computed using the logs up-scaled to the size of grid cells. Vertical variogram distances are expressed in fractions of grid thickness. Horizontal variograms are computed by considering pairs of points belonging to the same grid layer and with a tolerance angle of  $45^\circ$  and a bandwidth of 150m for each direction.

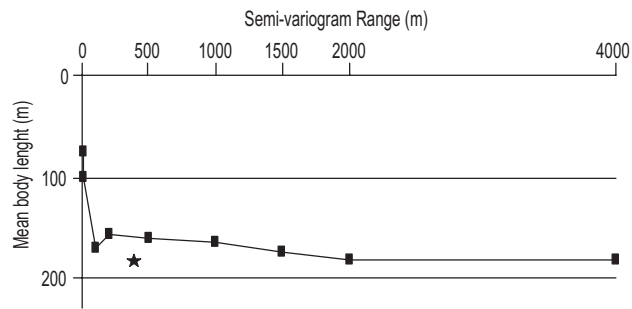


**Figure 6.** Plot of mean sand-dominated body length resulting for different horizontal variogram ranges using conditioned SIS for the 13A interval (vertical variogram ranges and proportions were kept constant, equal to those used for IK). Mean lengths represent the diameter of a cylinder with height set to the mean thickness extracted from well data (1.3m), with the same volume of each disconnected sand-dominated body. Results from 10 realizations are averaged for each semi-variogram range. Small undulations on the curve are explained due to the different effective proportions for each set of averaged realizations. Mean sand-dominated body size using IK with the fitted variogram is shown as a star.

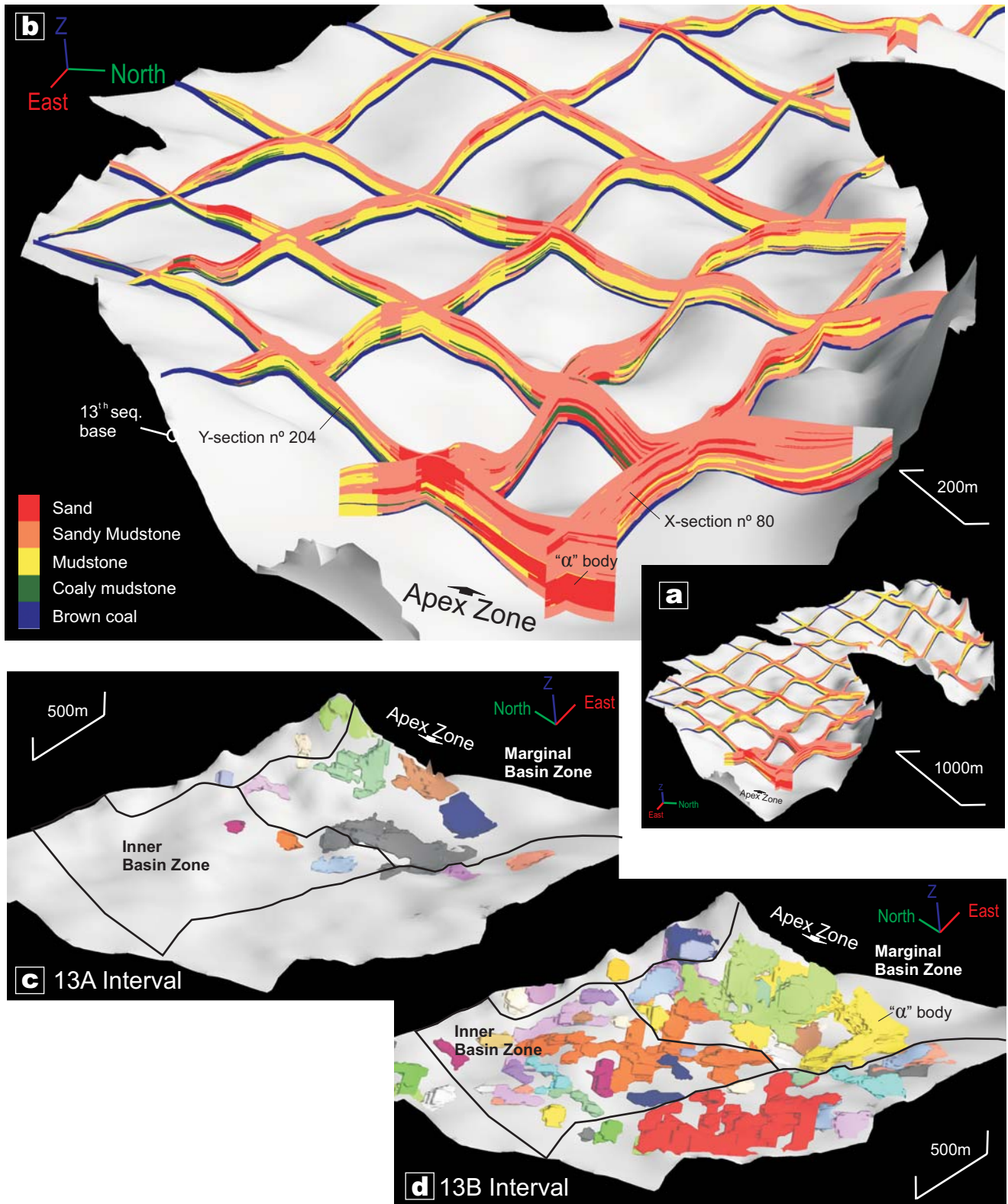


**Figure 7.** (a) Perspective view from the east of the facies reconstruction for the entire 13<sup>th</sup> sequence by showing several cross sections. (b) Detail of the axial alluvial fan. (c, d) Perspective view from the southwest of the enveloping surfaces for each laterally extensive sandstone body reconstructed in the basin. Each disconnected body has been distinguished with different color. Position of the axial alluvial fan apex zone is shown. Quantification has focused on the marginal basin zone and the inner basin zone where the axial alluvial fan developed. Note the perspective change from (a) and (b) to (c) and (d). Horizontal scales are approximate because of changes due to the perspective view, vertical exaggeration is x3.

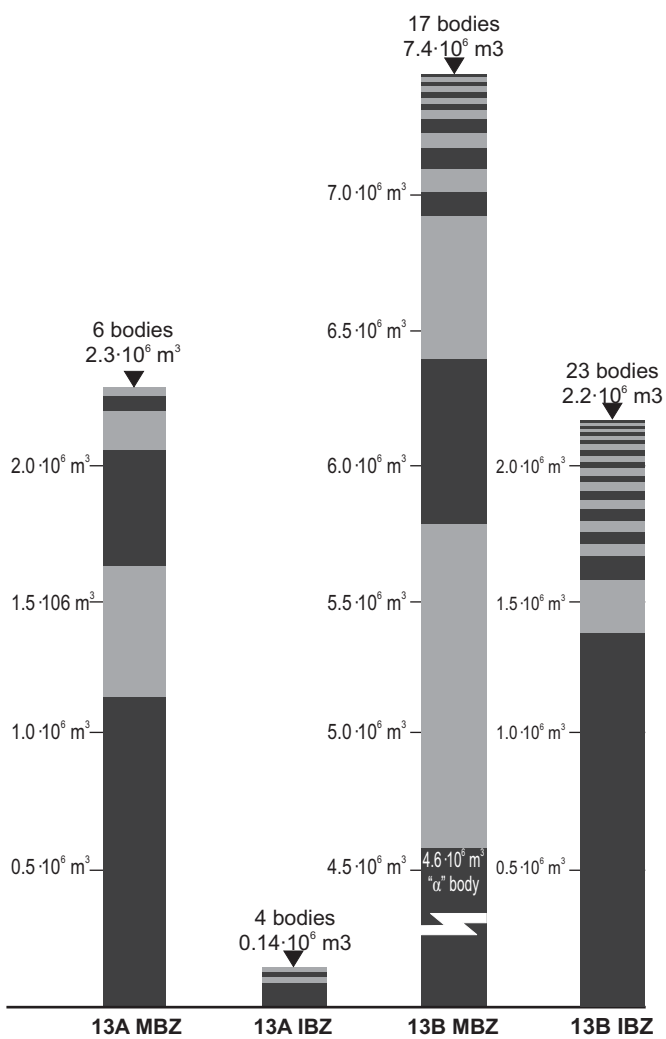


**Figure 8.** Bar graphs showing the volumes for each disconnected sand body analyzed in the Marginal Basin Zones (MBZ) and the Inner Basin Zones (IBZ) of the axial alluvial fan for the 13A and 13B interval. Note that the bar length for the largest body in 13B MBZ is not shown entirely in order to short the figure.

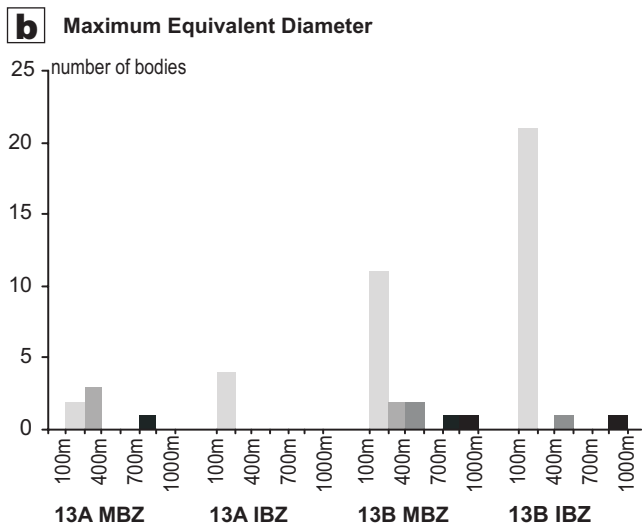
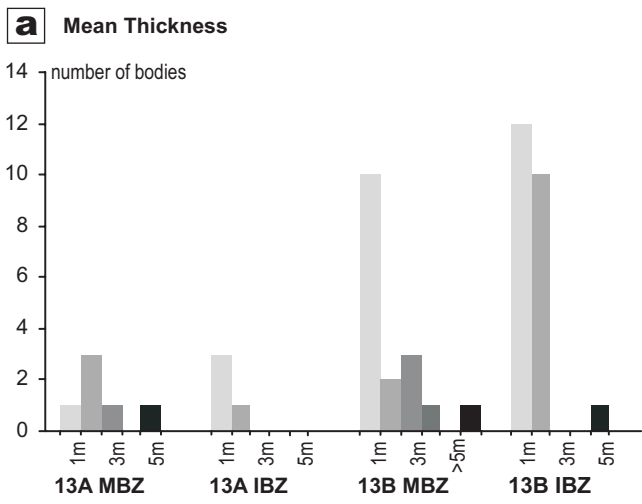
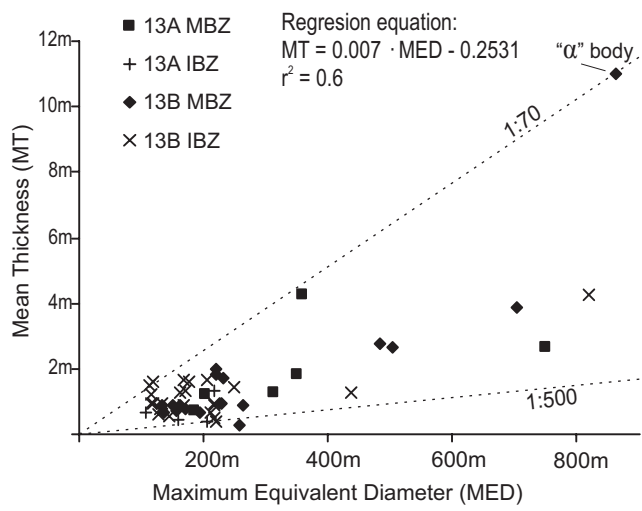


**Figure 9. (a, b)** Histograms for the mean thickness and maximum equivalent diameter for the disconnected sand bodies analyzed in the Marginal Basin Zones (MBZ) and the Intern Basin Zones (IBZ) of the axial alluvial fan for the 13A and 13B intervals.



		Variogram ranges			
		Horizontal		Vertical	
		13A Term	13B Term	13A Term	13B Term
AQUICLUDE FACIES	BROWN COAL	>150m.	-	> 0.1 > (0.7m-1.8m)	-
	COALY MUDSTONE	150m.	150m.	0.1 (0.7m – 1.8m)	0.16 (3m – 8.6m)
	MUDSTONE	300m.	>200m.	0.25 (1.8 – 4.5m)	> 0.24 > (4.6m – 13m)
	SANDY MUDSTONE	400m.	>200m.	0.3 (2.1m – 5.4m)	> 0.16 > (3m – 8.6m)
AQUIFER FACIES	SAND	400m.	250m.	0.3 (2.1m – 5.4m)	0.16 (3m – 8.6m)

**Table 1:** Horizontal and vertical variogram ranges fitted assuming a spherical model for each facies. Horizontal and vertical ranges for brown coal facies in 13A and mudstone and sandy mudstone facies in 13B are underestimated (see text for an extended explanation). Horizontal and vertical range for brown coal facies in 13B is not presented since coals are very scarce in this term (less than 0.5%). Because a grid with proportional layering is used the vertical ranges are expressed in fractions of the grid thickness, as grid thickness varies between different locations, the real vertical range also changes. In brackets there are approximate average values and maximum values for real vertical ranges expressed in meters.

		13A Interval	13B Interval
Marginal basin zone	Total volume	$13.9 \cdot 10^6 \text{ m}^3$	$44.8 \cdot 10^6 \text{ m}^3$
	Sand volume	$2.2 \cdot 10^6 \text{ m}^3$	$7.5 \cdot 10^6 \text{ m}^3$
	Sand percent	16%	17%
Inner basin zone	Total volume	$10.2 \cdot 10^6 \text{ m}^3$	$31.1 \cdot 10^6 \text{ m}^3$
	Sand volume	$0.2 \cdot 10^6 \text{ m}^3$	$3.1 \cdot 10^6 \text{ m}^3$
	Sand percent	1%	10%

**Table 2:** Total volume, sand volume and sand percentage for the 13A and 13B intervals and for the MBZ and IBZ where alluvial fan deposits dominated as extracted from the reconstruction.